^{14}C chronology and stable isotopes on Lymnaea viatrix *shells in northwest Patagonia, Argentina. Do they express the Antarctic climatic reversal?*

Héctor O. Panarello, Romina Sanci & Leonard I. Wassenaar

Carbonates and Evaporites

ISSN 0891-2556

Carbonates Evaporites
DOI 10.1007/s13146-018-0455-9

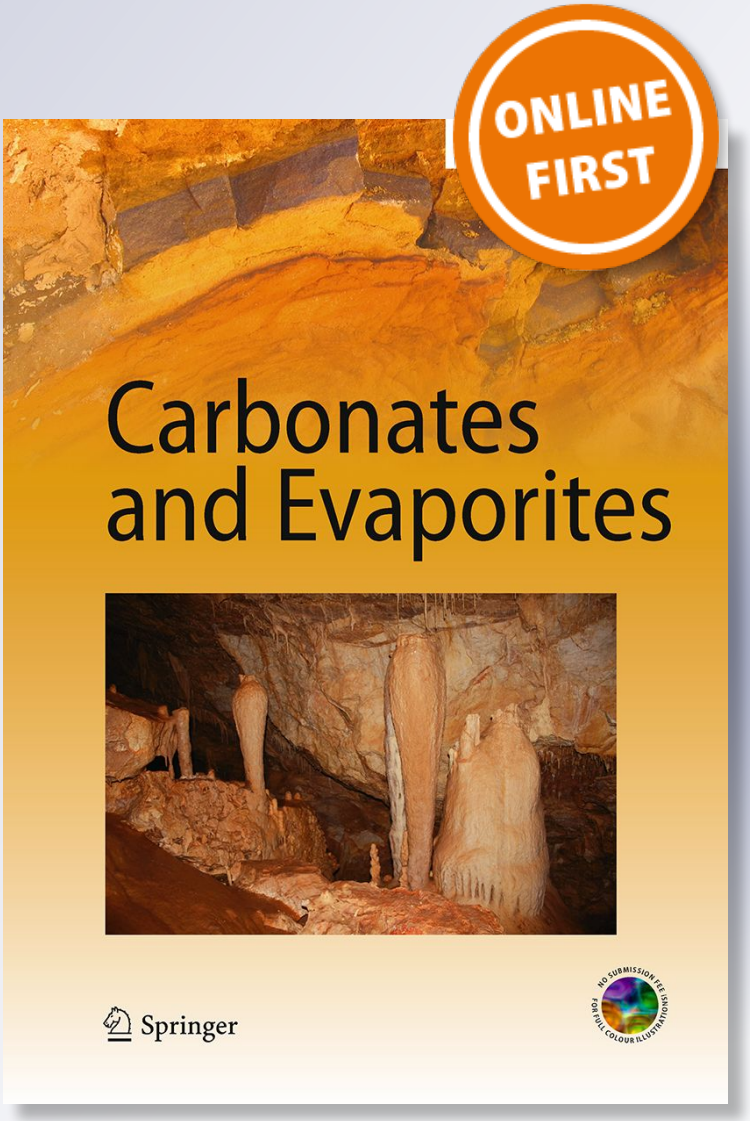

Springer

Carbonates and Evaporites
https://doi.org/10.1007/s13146-018-0455-9

ORIGINAL ARTICLE

^{14}C chronology and stable isotopes on *Lymnaea viatrix* shells in northwest Patagonia, Argentina. Do they express the Antarctic climatic reversal?

Héctor O. Panarello[1] · Romina Sanci[2] · Leonard I. Wassenaar[3]

Accepted: 20 June 2018

Abstract
A multi-isotope environmental record comprising an upper section of the late Pleistocene and the lower and middle Holocene, including isotopic data on 30 samples of peat, marl, tufa, *Lymnaea viatrix* shells, and *Hippidion sp*. teeth, is described from a 15 m profile at Arroyo Leuto Caballo, Neuquén Province, Argentina. The chronology of the Pleistocene sequence was derived from five modeled ^{14}C ages. δ^{18}O of *L. viatrix*, assumed as a proxy for δ^{18}O of meteoric water isotopic composition and thus sensitive to air temperature changes, showed a warming period from 14.03 cal ka BP until ca. 13.90 cal ka BP, followed by a rapid decline in temperature, attaining a minimum between 13.79 and 13.56 cal ka BP and a subsequent warming reestablishment. In addition, a "specular pattern" of δ^{13}C of *L. viatrix* peaking in the same time span would be probably showing aridity. This pattern developed within the globally defined Antarctic Cold Reversal-ACR-time span (from 14.6–2.8 cal ka BP), and prior to the onset of the Huelmo Mascardi Cold Reversal episode, HCMR, from ca 13.30–1.87 cal ka BP. Given the characteristics and the time span covered, it could be related to a continental expression of the ACR event.

Keywords Modeled ^{14}C ages · Stable isotopes · Continental carbonates

Introduction

The Patagonian glaciations began after the late Miocene (ca. 6 Ma) as multiple events of varied duration and intensity, including the Great Patagonian Glaciation (GPG; ca. 1 Ma) (Rabassa et al. 2011). The modern landscape, however, is a result of the late Pleistocene glaciation. The Patagonian glaciations have yielded evidence of several pre-GPG cold periods (between 7 and 2 Ma), three post-GPGs during the early and middle Pleistocene, the last glaciation (LG) with ice sheets reaching their maximum areas between 25 and 23 ka, and episodes of glacial stabilization during the late glacial (Coronato et al. 2004). Deglaciation occurred in 17.5 and 11.4 ka in South America (Sugden et al. 2005), opposite to the climatic changes in the northern mid- to high-latitudes during this interval (Shakun and Carlson 2010). The two major climatic transitions occurred in the North Atlantic region in 14.7 and 11.5 cal ka BP from the Oldest Dryas to the Bolling–Allerod interstadial, and from the Younger Dryas (YD) to Preboreal, respectively (Renssen et al. 2001). The conventional explanation for these divergent climate trends is a bipolar ocean seesaw effect, which is responsible for hemispheric coupling via oscillations in the dominant direction of heat transport in the Atlantic Ocean due to perturbations in the meridional overturning circulation (Newnham et al. 2012). Despite the differences, all available palaeoclimatic records show a similar pattern in southernmost South America region: an overall warming trend starting in 19 ka BP and interrupted by a millennial scale event called Antarctic Cold Reversal (ACR) (Pedro et al. 2011). Blunier et al. (1998) correlated with the Greenland GRIP and the

✉ Héctor O. Panarello
h-panarello@doctor.com

[1] Instituto de Geocronología y Geología Isotópica (Consejo Nacional de Investigaciones Científico Técnicas-Universidad Buenos Aires), Ciudad Universitaria, Intendente Güiraldes 2160, Pabellón INGEIS, C1428EHA Buenos Aires, Argentina

[2] Instituto de Geociencias Básicas, Aplicadas y Ambientales de Buenos Aires (Consejo Nacional de Investigaciones Científico Técnicas-Universidad Buenos Aires), Ciudad Universitaria, Intendente Güiraldes 2160, Pabellón II, Piso 1, C1428EHA Buenos Aires, Argentina

[3] Department of Nuclear Sciences and Applications, Vienna International Centre, International Atomic Energy Agency (IAEA), PO Box 100, 1400 Vienna, Austria

Published online: 04 July 2018

Antarctic Vostok and Byrd ice core records using methane to show that the ACR of the Southern Hemisphere preceded the YD of the Northern Hemisphere by at least 1800 years, and lasted from ca. 14.5–12.7 ka BP. While the ACR is well defined in ice core records from Polar Regions, its manifestation elsewhere in terrestrial environments (Andean and extra-Andean territory) is rare and inconclusive (Glasser et al. 2012; De Porras et al. 2014).

In Northern Patagonia, terrestrial evidence for glacial fluctuations is found in the Andes Cordillera (Rabassa 2008), and in palaeoclimatic proxies such as lakes and palynological records in the extra-Andean area. Mehl and Zárate (2014) showed evidence of alluvial paleosol sequences developed on Late Glacial aeolian deposits in the Andean Piedmont reflecting the climatic transition from arid (prior to ca. 10 ka BP) to warmer and more humid climatic conditions. At Mallín Vaca Lauquen, the Late Glacial–early Holocene pollen records show cooler and drier summers than present (Markgraf et al. 2009). A major climatic shift to more arid conditions occurring after 24 ka is documented by significant aeolian activity in the Andean Piedmont of Central Mendoza, with an interval from 16 to 13 ka, related to arid and cold environmental conditions (Tripaldi et al. 2011). In Southernmost Patagonia, palynological records confirm arid conditions between 13.0 and 11.3 ka (Bamonte and Mancini 2011; De Porras et al. 2014). Records of pollen, charcoal, wood, and organic carbon from southern mid-latitude lakes of the east side of the Andes suggest a cool episode before the onset of the YD. Moreno et al. (2009) reported evidence (from fen, bog and lakes) of a cold episode between 14.8 and 12.6 ka and a glacial re-advance in south-western Patagonia, contemporaneous with the ACR.

In this paper, new terrestrial palaeoclimatic isotope and radiocarbon data are documented to provide evidence of changes in environmental conditions, probably related to the ACR. These records were obtained from sediments at several depths (peat, marl, and tufa), shells of continental molluscs (*Lymnaea* sp.), and *Hippidion* sp. teeth from a Patagonian site (~ 37°10′S; ~ 70°10′W). To establish a reliable chronology, the modeling of ^{14}C ages by Panarello and Fernández (1999) was reinterpreted. ^{18}O variations in sediments and shells were related to temperature changes, and ^{13}C changes in the vegetal cover were induced by environmental changes.

Study area

The Arroyo Leuto Caballo site is located in north-western Patagonia, Neuquén Province, and to the north of Chos Malal city in the neighborhood of the basaltic Pun Mahuida or Tromen Volcano (4114 m a.s.l.), Argentina (Fig. 1). The mean elevation is ~ 1300 m a.s.l. The region is currently semiarid with poor vegetation cover, mainly as shrubs and bushes. Precipitation related to the Pacific Anticyclone passes over the Andean barrier and shows a gradient from West to East (Panarello and Dapeña 2009), reaching 600 mm/year in the Western zone and 200 mm/year in the lower eastern zone (Chos Malal, 263 mm/year), mainly in winter (https://es.climate-data.org). At present, predominant winds are from W and S in summer and from W in winter. The Arroyo Leuto Caballo drains to the Neuquén River basin, which receives inputs from other minor rivers and arroyo systems. Snowmelt allows the development of an important hydrological network via the Colorado and Neuquén rivers, which drain to the Atlantic Ocean.

Geomorphological analysis of the study area shows that the present relief was formed by glacial action, volcanic activity, and fluvial and landslide processes (Gonzalez Diaz and Folguera 2011). In valleys, more recent deposits are exposed by the current fluvial erosion. The erosion formed ravines whose escarpments reach a vertical development of 15 or more meters, like in the study area. The geological setting corresponds to the Neuquén Basin formed by Mesozoic marine sedimentary rocks, intrusive bodies, Pliocene–Quaternary volcanic ash, and rocks (basalts) from the intense Cenozoic magmatic activity, and clastic sinorogenic deposits (Sánchez et al. 2014; Sagripanti et al. 2014). Quaternary sediments, Cretaceous to Paleogene marine and continental deposits, and Paleogene to Neogene volcanic and subvolcanic rocks are crossed by the Leuto Caballo stream (Fig. 1).

Particularly, the Arroyo Leuto Caballo geologic profile contains sediments from the late Quaternary to present (Panarello and Fernández 1999). Lithology consists of tufa, marl, and peat deposits with the presence of fossils. The oldest beds of organic-rich material contain extinct Pleistocene vertebrate fauna, mainly *Equidae* (*Hippidion* sp.) and *Macraucheniidae* (*Macrauchenia*), fragmented in a way that suggests water transport into a peat bog. No vertebrate animal remains have been found in the Holocene strata. It was suggested that the fossils represent an episode of Pleistocene South American mega-faunal mammal extinction, since there is no evidence of human handling or marrow extraction. Neither lithic materials, coal, nor human relics have been found. However, a fish tail projectile tip was found 20 km from this site, which represents an excellent marker indicating the presence of earlier hunter-gatherer populations living during the end of the Pleistocene and its transition to the Holocene (Patané Aráoz and Nami 2014). There is abundant invertebrate fauna of *Gastropoda* (*Lymnaea aff. viatrix*) in the overall profile. Unfortunately, it is not evenly distributed and large sections of the Holocene show no fauna. The marl contains up to 80% $CaCO_3$ according to X-ray diffraction analyses (Rozanski 1995). Volcanic ash was observed at 8.94 m below ground surface.

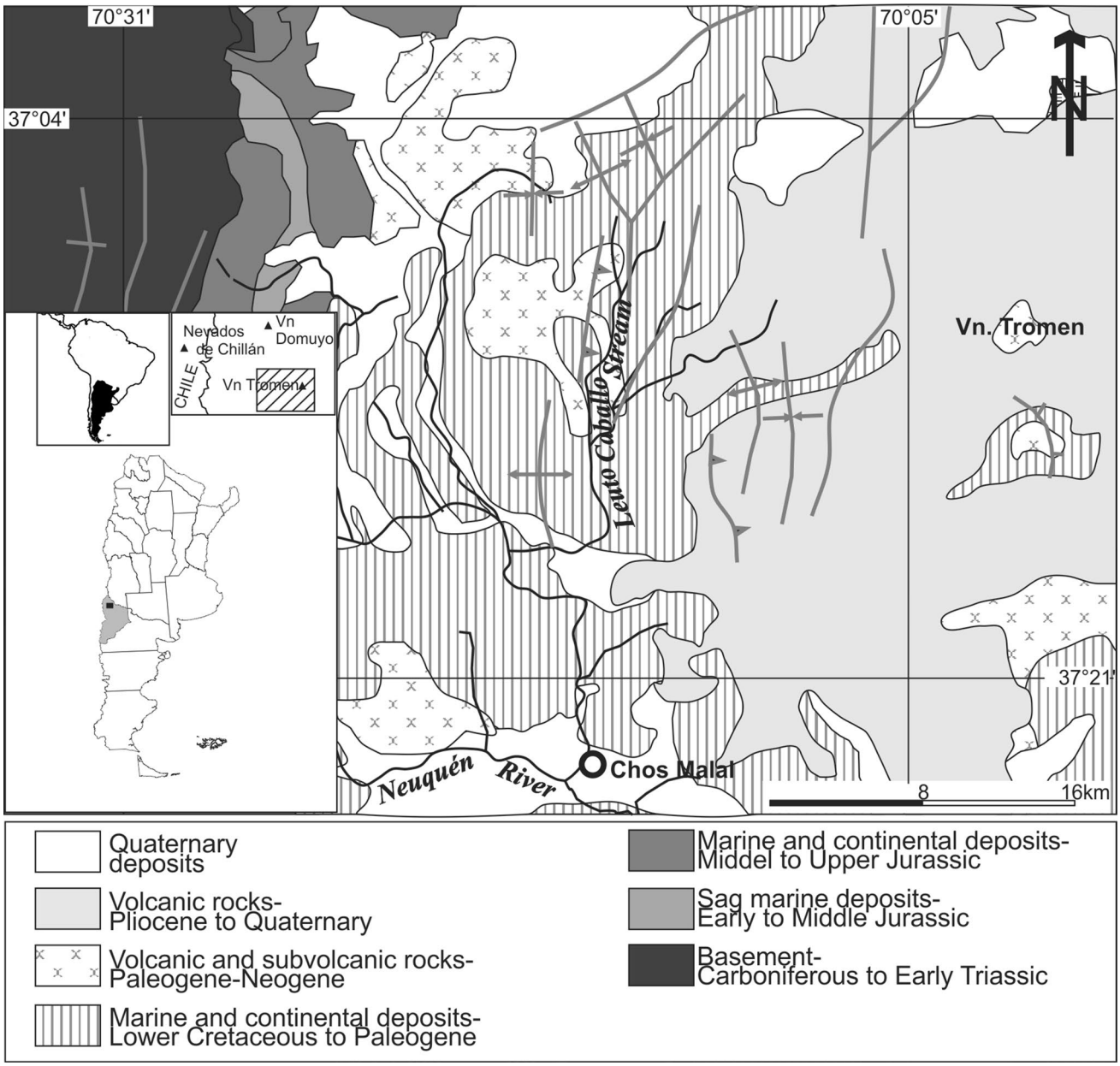

Fig. 1 Location map showing Arroyo Leuto Caballo, Neuquén Province, Argentina. Simplified geologic map of study area (modified of Sagripanti et al. 2014)

Materials and methods

28 samples of carbonates (tufa and marl) and *L. viatrix* shells were analyzed for $\delta^{13}C$ and 10 ^{14}C dates were obtained along a ca. 15 m vertical profile. Two $\delta^{18}O$ values from teeth of *Hippidion sp.* found in peat in the 13–14 m interval were also measured. To assess the ^{14}C chronology, an OxCal deposition model was used (Bronk Ramsey and Lee 2013). The model was ran for the Pleistocene section using Poisson, P sequence, a null reservoir effect, $\Delta R = (0 \pm 600)$ years, by means of SHCal13 (Southern Hemisphere curve; Hogg et al. 2013), and a general outlier model. The media (μ) of the age intervals was used to calculate mean deposition rates.

For ^{14}C dating of tufa, marl, and peat, samples were pretreated to remove exogenous material such as organic matter in carbonates and modern roots and carbonates in peat. Dating was performed at the Instituto de Geocronología y Geología Isotópica (INGEIS) laboratories by liquid scintillation counting by benzene synthesis. Carbonate samples were treated with concentrated $HClO_4$, and peat was combusted in O_2 stream in the presence of CuO. In both cases, the evolved CO_2 was cryogenically purified and reduced to

CH≡CH with lithium at 900 °C. CH≡CH was then trimerised to benzene with a Perlcator® chromium oxide catalyser. POPOF in toluene, scintillation liquid, was then added to 10 mL of each sample, which was measured in a Packard TRICARB® 4530 for 1000 min of counting (Leger and Tamers 1963). ^{14}C analysis on *L. viatrix* was performed by Accelerator Mass Spectrometry (AMS), at the Australian National Nuclear Research and Development Organization (ANSTO) facility, Australia.

Stable isotopes of carbonates were measured at INGEIS laboratories, according to McCrea (1950) and further modifications (*v. gr.* Panarello et al. 1980). Samples were ground to 100–200 µm, and heated to 350 °C in vacuo to eliminate organic matter, then treated with 100% phosphoric acid in vacuo (10^{-2} Pa) at 80 °C in a thermostatic bath. The CO_2 was cryogenically purified and measured for $\delta^{13}C$ and $\delta^{18}O$ using a Finnigan Delta-S dual inlet mass spectrometer, together with the internal standards INGEIS-1-Carrara marble ($\delta^{13}C = 2.2‰$; $\delta^{18}O = 29.4‰$) and INGEIS-2–SJ-metamorphic calcite ($\delta^{13}C = -0.8‰$; $\delta^{18}O = 13.72‰$). Isotopic values enrichments are expressed in the $\delta^{13}C$ and $\delta^{18}O$ notation in permil (‰) vs. the VPDB and VSMOW reference standards (Craig 1957; Gonfiantini 1978). The overall analytical uncertainty was ± 0.1‰. Oxygen isotopes on two *Hippidion* teeth's enamel were determined at the Universitá degli Studi, Trieste, Italy (A. Longinelli, personal communication, 1995), and the results are given as the isotopic composition of correlated meteoric water.

Results and discussion

Table 1 contains the conventional radiocarbon ages BP (years before 1950) for ten samples of the profile, covering the time span from 12200 to 2720 BP, along with $\delta^{13}C$ and $\delta^{18}O$ values for tufa, marl, peat, *L. Viatrix*, and *Hippidion* teeth (only $\delta^{18}O$) samples and the corresponding isotopic composition of source meteoric water ($\delta^{18}Ow$). The $\delta^{18}O_w$ for "inorganic carbonates" IC (tufa and marl) ranged from −11.7 to −10.2‰, while *L. Viatrix* $\delta^{18}O_w$ fluctuated between −5.5 and −3.8‰. Water drunk by *Hippidion* (in equilibrium with teeth enamel found in peat) yielded $\delta^{18}O_w$ values of −12.2 and −10.4‰. $\delta^{13}C$ from tufa and marl varied between −9.0 and −8.0‰ and *L. viatrix* between −8.0 and −5.6‰. These variations in $\delta^{18}O_c$ and $\delta^{13}C_c$ with depth for carbonates and *L. viatrix* shells are represented in Fig. 2.

Isotopic analyses of terrestrial carbonates are suitable for studies of the late Pleistocene and Holocene, taking into account that carbonates often preserve continuous records of accumulation, and correlate with $\delta^{18}O$ of the water and $\delta^{13}C$ of DIC from which calcite precipitate (Andrews 2006; Sharp 2007). In the case of the Leuto Caballo site, the $\delta^{18}O$ of both IC (tufa and marl) seem to be in equilibrium with meteoric water occurring in the nearby area, since $\delta^{18}O_w$ values resemble those of modern precipitation in the zone, whose $\delta^{18}O$ values range from ca. −14 to −10‰ due to changes in air temperature and altitude (Panarello 2002; Panarello et al. 1992). For instance, the Colorado River, collector of the drainage network, shows at present (2002–2007 period) a mean $\delta^{18}O = -12.45‰$. Besides, continental deposits from temperate regions, such as lake marls, with low salinity, and shallow water conditions, can record either the isotopic trends or the residence time of water in the pond (Turner et al. 1983; Treese and Wilkinson 1982). With long residence times, gas exchange with the CO_2 atmospheric pool ($\delta^{13}C$ ca. −8‰ at present, but ~ −6.5‰ before the XIX century) and evaporation combine to enrich DIC in ^{13}C and water in ^{18}O. With short residence times, waters retain the original $\delta^{18}O$ of the meteoric water and the $\delta^{13}C$, that of the soil gas CO_2 initially dissolved (DIC) in the water inflowing the lake ($^{13}\varepsilon HCO_3\text{-}/CO_2$ ca. +9‰ at 15 °C). Therefore, the similarity between $\delta^{18}O_w$ of IC source water and $\delta^{18}O$ values in present waters from Leuto Caballo would suggest water with low residence time. Moreover, since $\delta^{18}O$ of tooth enamel closely resembles the isotopic composition of local meteoric water in equilibrium with the body temperature of the warm blooded mammal (Longinelli 1984), it is assumed that $\delta^{18}O_w$ values of *Hippidion* and IC are reflecting the same environmental changes.

Shell carbonate from freshwater environments is often adequate for isotopic paleoclimatological studies, since long-term fluctuations in oxygen isotopes may be preserved in stratigraphic successions of shell material grown in the water. *L. Viatrix* lives in stagnant and slow circulating waters (Deis et al. 2008), similarly to *L. Stagnalis*, that was defined as a suitable indicator for variations in water ^{18}O composition (Fritz and Poplawsky 1974). In the Leuto Caballo site, *L. viatrix* shells were found in tufa, marl, and peat strata, confirming shallow freshwater environments.

Comparing the $\delta^{18}O$ values of *L. viatrix* and carbonates, isotopic differences were observed along the depth profile. In the upper end of the section, up to ~ 3 m deep, *L. viatrix* and carbonates showed a similar pattern with differences close to −8‰. Unfortunately, the lack of *L. viatrix* between 3 and 8 m deep did not allow for further comparisons. Below 8 m deep, despite the lack of resolution of the IC sampling and the scarceness of *L. viatrix,* $\delta^{18}O$ records for both retained the same average difference of ca. −8‰. Regarding $\delta^{13}C$, IC samples also showed a systematic depletion in of about 2‰ when compared to *L. viatrix*.

Differences in the oxygen and carbon isotopic composition between *L. viatrix* and IC could be explained as follows. Given the shallow ponds that prevailed in the study area, with $\delta^{18}Ow$ of IC indicating a low residence time, it is possible to suggest that IC also resulted from the DIC of surface runoff or phreatic water feeding the pond in equilibrium

Table 1 Depth, $\delta^{13}C$, $\delta^{18}O_c$, $\delta^{18}O_w$ ^{14}C age, and material type for the analyzed samples

Stable isotope#	^{14}C lab#	Depth (m)	$\delta^{13}C$(‰) V−PDB (‰)	$\delta^{18}O_C$ ‰ V−SMOW (‰)	δ^{18}Ow‰ V−SMOW*	^{14}C age (BP) (ka BP)	Analysis on
AIE5688		1.80	−6.3	26.4	−4.0		*Lymnaea* (tufa)
AIE3780		2.10	−8.7	19.1	−11.1		Tufa
AIE5689		2.20	−6.4	25.9	−4.5		*Lymnaea* (tufa)
AIE3869	AC1252	2.30	−8.8	18.7	−11.5	2720 ± 90	Tufa
AIE3866		3.00	−8.0	18.5	−11.7		Tufa
AIE5690	OXB356U	3.00	−5.6	25.8	−4.6	2880 ± 50	*Lymnaea* (tufa)
AIE3868	AC01251	3.70	−9.0	18.5	−11.7	5635 ± 120	Tufa
AIE3867		4.30	−8.2	18.7	−11.5		Marl
AIE3865		5.10	−9.0	19.3	−10.9		Tufa
AIE3864		6.00	−8.7	19.3	−10.9		Tufa
AIE3862	AC1249	7.40	−8.7	19.7	−10.5	8445 ± 150	Tufa
AIE3861		7.60	−9.1	19.8	−10.4		Tufa
AIE5691	OXB355U	7.72	−6.9	26.1	−4.3	8760 ± 60	*Lymnaea* (tufa)
AIE5692		8.94	−6.6	26.1	−4.3		*Lymnaea* (ash)
AIE5693		9.32	−6.5	26.6	−3.8		*Lymnaea*
AIE5694		9.57	−6.0	26.2	−4.2		*Lymnaea* (marl)
AIE3859	AC1250	9.60	−7.6	19.6	−10.6	10,100 ± 300	Marl
AIE3860a		11.75	−8.1	20.0	−10.2		Marl
AIE3860b		11.75	−6.1	26.1	−4.3		*Lymnaea* (marl)
AIE3863		12.00	−8.9	19.3	−10.9		Marl
AIE3863		12.25	−6.8	19.9	−10.3		Marl
AIE5695	OXB354U	12.88	−7.2	26.2	−4.2	11,650 ± 70	*Lymnaea* (marl)
	AC0981	13.00	−23.5			11,940 ± 200	Peat
T2		13.00			−12.2		Tooth* (peat)
AIE5696		13.07	−5.9	24.9	−5.5		*Lymnaea* (peat)
AIE5697		13.53	−5.9	24.9	−5.5		*Lymnaea* (peat)
AIE5698		13.77	−8.0	26.5	−3.9		*Lymnaea* (peat)
AIE5699	OXB353U	14.01	−7.2	26.0	−4.4	12,200 ± 80	*Lymnaea* (peat)
	AC0980	14.01	−23.0			12,200 ± 200	Peat
T1		14.01			−10.4*		Tooth* (peat)

*18Ow of the source water in equilibrium with carbonate or yooth enamel

with meteoric water and soil CO_2. Water evaporated in the pond to dryness, leaving a stratum with an isotopic composition identical to that of DIC. On the other hand, *L. viatrix* shells are enriched in ^{18}O and ^{13}C. The ^{13}C content of shells could be related to the short turnover time of the pond that allowed CO_2 isotopes to attain only partial equilibrium with the atmospheric pool, leading to less negative values (Fritz and Poplawsky 1974). $\delta^{18}O$ of shells is the result of the equilibration with an average isotopic composition of water during a Rayleigh evaporation process. It is assumed that *L. Viatrix* was growing while water was present, being the δ^{18}Ow determined by the equation: $\delta = \delta° + \varepsilon \ln F$, where $\delta = \delta^{18}O_w$ at a given time, $\delta° = \delta^{18}O_w$ when the pool is replenished, ε = enrichment factor (ca. 9‰), and F = W/W° remaining water volume (Dansgaard 1961, 1964). Thus, carbonate would precipitate in equilibrium with a progressively enriched reservoir. This would lead to an enrichment of ca 8.5‰ with $1 > F > 0.2$. In *L. Viatrix*, the enrichment was less than ≈6‰, due to the input of new meteoric waters during the process. Therefore, *Lymnaea* is reflecting the conditions in the pond, and IC, in the water coming from surrounding areas.

The $\delta^{18}O$ record in IC ends at a depth of ca. 12 m, although it is continued in the two *Hippidion* sp. teeth to the end of the profile. In the Late Pleistocene section (bellow 12 m deep), *L. viatrix* sampling had a better time resolution and showed a different pattern for $\delta^{18}O$ and $\delta^{13}C$. Therefore, the ^{14}C dates available for this section were chosen to run the age-depth model. The OxCal deposition model (Bronk Ramsey and Lee 2013) for the Pleistocene

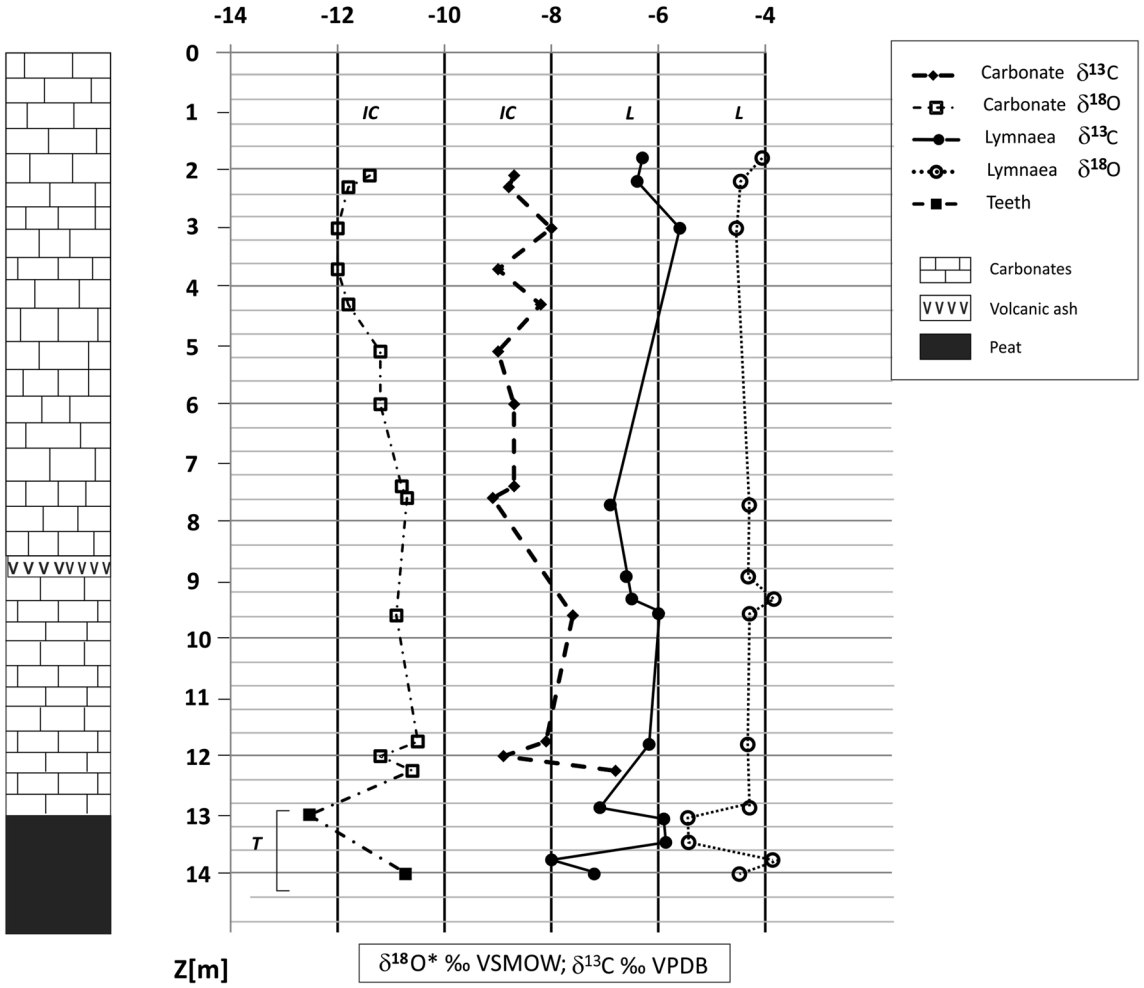

Fig. 2 Stratigraphic distribution of isotopic data ($\delta^{18}O$ and $\delta^{13}C$ on carbonates, *Lymnaea* and *Hippidion* teeth)

section yielded calibrated ^{14}C ages (95.4%) that ranged from 14.25 to 10.78 cal ka BP (Table 2). Taking these results as prior likelihood, the model generated a 14.22 to 11.10 ka modeled interval. A sample of *L. viatrix* and a sample of peat corresponding to a depth of 14.01 m, constituted the lower boundary of the profile. Both samples gave the same ^{14}C age (12200 BP), but the *L. viatrix* age had lower uncertainty. The model combined them in

Table 2 Calibrated and modeled ages (2σ, 95.4%)

Name	Calibrated (BP)				Modeled (BP)						
	From	To	μ	σ	From	To	μ	σ	Index		
									A	P	C
*R*_Date 960	12,635	10,781	11,696	464	12,619	11,096	11,794	387	107.7	96.0	95.4
*R*_Date 1288	13,571	13,292	13,434	76	13,580	13,324	13,462	68	105.3	96.6	99.8
*R*_Date 1300	14,322	13,283	13,790	262	13,664	13,375	13,527	73	95.9	96.2	99.7
*R*_Combine 1401P/1401L	14,247	13,771	14,028	128	14,219	13,793	14,025	109	107.2	96.5	99.5
*P*_Sequence (1,0.2,U(-2,2))	− 2	2	0	11,431	− 1.6	2.02	0.231245	106,114	100.0		99.1
U(0,4)	0	4	2	11,431	0	4	192183	113,938	100.0		99.8

A_{model} 107.4%, $A_{overall}$ 106.5%. See Bronk Ramsey (2008)

A agreement, *C* convergence, *P* Bayesian posterior probability distribution,

one sample ($R_{combine}$ 1401P/1401L). The age-depth model (ADM; Fig. 3) yielded mean deposition rates for the Pleistocene by plotting the media vs. depth showing a perfect correlation:

$$\text{Age [ka BP]} = 0.507\ Z\ [\text{m}] + 6.93\ \text{ka};\ R^2 = 1.000. \quad (1)$$

Shifts between modeled and calibrated ages were related to reservoir effects. Aragonite of *L. viatrix* shells did not show any isotopic shift, only *R*_date 1300 (peat) is aged by 263 years, probably due to incomplete elimination of old carbonates during pre-treatment.

Since the age-depth model for the Pleistocene segment (Fig. 3) gave a reliable chronology for this temporal interval and allowed estimating the mean deposition rate, we calculated ^{14}C age of six samples of *L. viatrix* at 14.01, 13.77, 13.53, 13.07, 12.88, and 11.75 m using Eq. (1) (Fig. 4). These samples showed ^{18}O enrichment between 14.03 and 13.91 cal ka BP, interrupted by a sharp decrease, beginning in 13.91 cal ka BP, following in 13.79 cal ka BP, lasting till 13.56 cal ka BP, and resuming the increase toward 13.46 cal ka BP. Values of $\delta^{13}C$ for *L. viatrix* decreased 0.8‰ from 14.03 to 13.91 cal ka BP, followed by a rapid

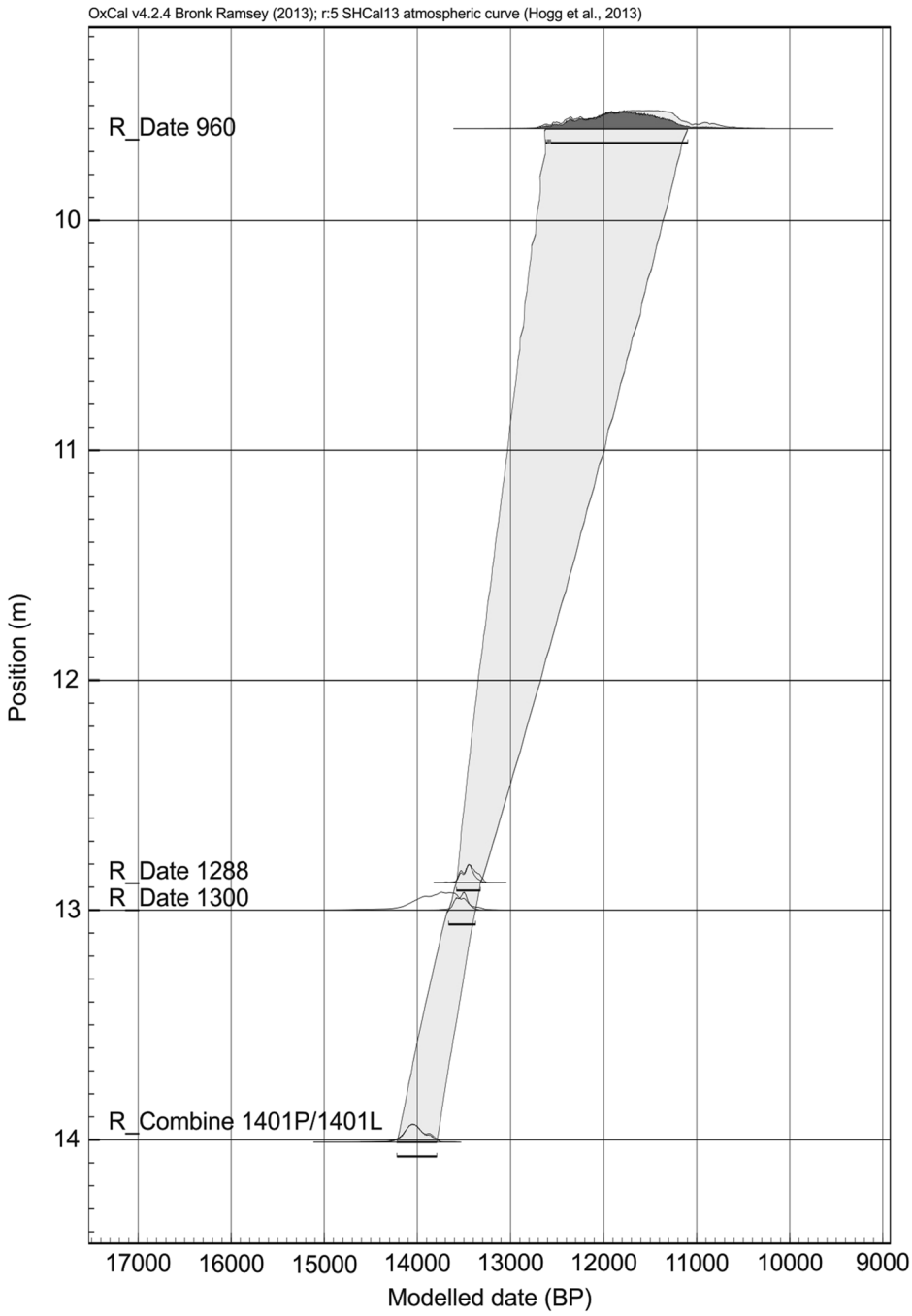

Fig. 3 Age-depth model for the Pleistocene section constructed using five radiocarbon dates

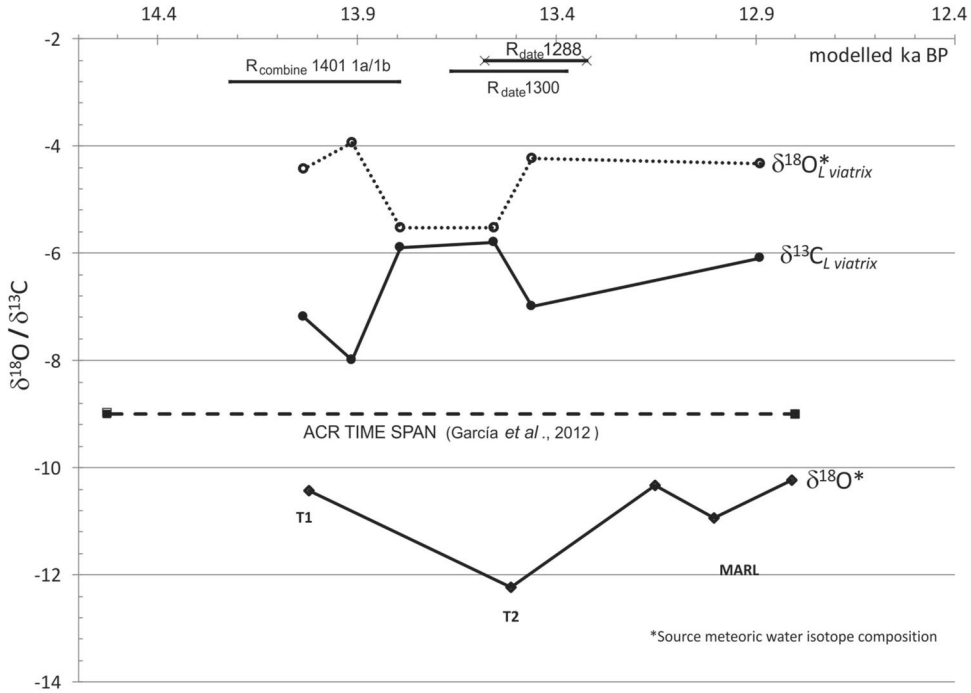

Fig. 4 Evolution of carbon and oxygen isotope composition of *Lymnaea*'s carbonate, during the ACR time span indicating warmer and dryer conditions during at least 400 years in the centre of the interval. *Hippidion* enamel oxygen-18 showed a similar trend

increase of 2.1‰ until 13.56 cal ka BP and descending 1.1‰ at 13.46 cal ka BP, showing a specular pattern when compared to $\delta^{18}O$. In Fig. 4, $\delta^{18}O$ values from water in equilibrium with the two *Hippidion* teeth at 14.03 and 13.52 cal ka BP are shown. The curve is in agreement with $\delta^{18}O$ of three marls at 13.15, 13.00 and 12.81 cal ka BP. In Fig. 3, an ash layer occurring at 8.94 m was dated using (1) to 11.5 cal ka BP.

If $\delta^{18}O$ of *L. viatrix* reflected air temperature changes through the isotope composition of meteoric water, a warming period from 14.03 cal ka BP till ca. 13.9 cal ka BP could be inferred, followed by a rapid decrease in temperature, reaching a minimum between 13.79 and 13.53 cal ka BP, and then resuming the warming trend. The positive $\delta^{13}C$ excursion was probably due to a higher C_4/C_3 ratio in the vegetal cover or to a photosynthetic pathway switching from C_3 to CAM in response to hydric stress (Farquhar et al. 1989). This is reflected in the DIC's $\delta^{13}C$ of groundwater inflowing the pond and consequently in *L. Viatrix* $\delta^{13}C$. Pollen evidence (Iglesias et al. 2014) at La Zeta Lake, Argentina, south of the study area, revealed changes in this direction. Around 13.9 cal ka BP, it showed an important reduction in *Nothofagus* sp. (C_3) and an increase in *Poaceae* (mainly C_4, as recognized in Panarello and Sánchez 1985). Whitlock et al. (2006) described that shifts in sediment size and organic carbon were used to deduce relatively warm conditions prior to ca. 14.5 cal ka BP, followed by cool dry conditions that intensified between 13.3 and 11.7 cal ka BP. These authors expressed that all evidences discarded the possibility of this being a South American expression of the YD interval. Hajdas et al. (2003) had termed this period as the Huelmo/Mascardi Cold Reversal (HMCR), from ca. 13.30 to 11.87 cal ka BP. Bianchi and Ariztegui (2012) also observed that in the Río Manso Superior catchment area, inflowing in the NW area of the Mascardi Lake, an increase in steppe and high Andean semi-desert herbs, as well as *Poaceae*, at expenses of *Nothofagus* after 13.7 cal ka BP, started earlier than the major changes in the sedimentological record attributed to the HMCR.

$\delta^{18}O$ and $\delta^{13}C$ of *L. viatrix* would thus signal a return to cooler and dryer conditions, lasting ca. 500 a. Taking into account the $\delta^{18}O$ values drop and the counter phase signal of ^{13}C, associated with drier environments, observed during the time span (13.91–13.46) cal ka BP, it is reasonable to infer this as evidence of a signal related to the Antarctic Climatic Reversal (ACR) within the (14.6–12.8) cal ka BP interval (García et al. 2012) preceding the onset of the HMRC. The evolution of ^{18}O of *Hippidion* teeth and marl (Fig. 4) points to the same temperature trend, although with lower resolution.

Conclusions

In the study area in NW Patagonia, $\delta^{18}O$ of *L. viatrix*, assumed as sensitive for $\delta^{18}O$ of meteoric water isotopic composition and thus proportional to air temperature changes, suggested a warming period from 14.03 cal ka BP till ca. 13.9 cal ka BP. It was followed by a rapid cooling,

reaching a minimum at about 13.55 cal ka BP, resuming the warming at 13.4 cal ka BP.

A counter phase pattern of $\delta^{13}C$ values, attaining the least negative value for the late Pleistocene section, was interpreted as more arid conditions toward 13.55 cal ka BP. These circumstances would have induced a turnover in the flora to a higher C_4/C_3 plants ratio. Another possibility is a C_3 to CAM switching in their photosynthetic cycles caused by hydric stress. Both options would be reflected in $\delta^{13}C$ of the water DIC.

The evolution of $\delta^{18}O$ of *Hippidion* teeth and marl in the same time span, would be pointing to the same trend as $\delta^{18}O$ of *L. Viatrix*, although with lower resolution.

The OxCal deposition model has allowed detecting and placing in time an "anomalous isotopic signal" in a precise time span, older than 13.5 ka BP, and beyond the Pleistocene–Holocene limit (11.7 ka). This "anomalous isotopic signal" is situated in the middle of the time span assigned to the ACR defined within (14.6–12.8) cal ka BP and prior to the onset HMRC ca (13.30–11.87) cal ka BP.

Regarding the tufa and marl record, they have proven to be a suitable proxy for the meteoric water isotope composition and its palaeoenvironmental implication. However, the sampling resolution for the entire profile was too low to establish an association with other known paleoclimatic events occurring elsewhere.

Acknowledgements The authors are indebted to the Agencia de Promoción Científica y Tecnológica Argentina (ANPCyT) BID 802-OC AR PID 0535 project and to the International Atomic Energy Agency (IAEA), Research Contract 7117/RB, within the framework of the CRP "Continental Indicators of Paleoclimate" for their financial support. This work is dedicated to the memory of Jorge Fernández (1943–2001) and Susana Valencio (1955–2005) former responsible of the Stable Isotopes Laboratory of the INGEIS. We also thank Dr. Kazimierz Rozanki (University of Science and Technology in Kraków, Poland, Faculty of Physics and Applied Computer Science) for his valuable comments.

References

Andrews JE (2006) Palaeoclimatic records from stable isotopes in riverine tufas; synthesis and review. Earth Sci Rev 75:85–104

Bamonte FP, Mancini MV (2011) Palaeoenvironmental changes since Pleistocene-Holocene transition: pollen analysis from a wetland in southwestern Patagonia (Argentina). Rev Palaeobot Palynol 165:103–110

Bianchi MM, Ariztegui D (2012) Vegetation history of the Río Manso Superior catchment area, Northern Patagonia (Argentina), since the last deglaciation. Holocene 22:1283–1295

Blunier T, Chappellaz J, Schwander J, DaÈllenbach J, Stauffer B, Stocker TF, Raynaud T, Jouzel J, Clausen HB, Hammer CU, Johnsen J (1998) Asynchrony of antarctic and greenland climate change during the last glacial period. Nature 394:739–743

Bronk Ramsey C (2008) Deposition models for chronological records. Quat Sci Rev 27:42–60

Bronk Ramsey C, Lee S (2013) Recent and Planned Developments of the Program Oxcal. Radiocarbon 55:720–730. Oxcal 4.2.4. Electronic Resource https://journals.uair.arizona.edu/index.php/radiocarbon/article/viewFile/16215/pdf

Coronato AMJ, Martinez O, Rabassa J (2004) Glaciations in Argentine Patagonia, southern South America. In: Ehlers J, Gibbard P (eds) Quaternary glaciations: extent and chronology. Part III: South America, Asia, Africa, Australia and Antarctica. Elsevier, Amsterdam, pp 49–67

Craig H (1957) Isotopic standards for carbon and oxygen and correction factors for mass-spectrometric analysis of carbon dioxide. Geochim Cosmochim Acta 12:133–149

Dansgaard W (1961) The isotopic composition of natural waters. Medd Grønl 165:1–120

Dansgaard W (1964) Stable isotopes in precipitation. Tellus 16:436–468

De Porras ME, Maldonado A, Quintana FA, Martel-Cea A, Reyes O, Méndez C (2014) Environmental and climatic changes in central Chilean Patagonia since the Late Glacial (Mallín El Embudo, 44 S). Clim Past 10:1063–1078

Deis E, Sidoti L, Cuervo P, Marchesi V, Imbesi G, Gómez Rueda L, Mera y Sierra RL (2008) Caracterización ambiental de sitios con presencia de *Lymnaea viatrix* en la provincia de Mendoza, Argentina. Colegio Médico Veterinario de la provincia de Córdoba, Córdoba, Argentina

Farquhar GD, Ehleringer R, Hubic KT (1989) Carbon isotope discrimination and photosynthesis. Annu Rev Plant Physiol Plant Mol Biol 40:503–537

Fritz P, Poplawsky S (1974) ^{18}O and ^{13}C in the shells of freshwater mollusks and their environments. Earth Planet Sci Lett 24:91–98

García JL, Kaplan MR, Hall BL, Schaefer JM, Vega RM, Schwartz R, Finkel R (2012) Glacier expansion in southern Patagonia throughout the Antarctic Cold Reversal. Geology 40:859–862

Glasser N, Harrison S, Schnabel C, Fabel D, Janson KN (2012) Younger Dryas and early Holocene age glacier advances in Patagonia. Quat Sci Rev 58:7–17

Gonfiantini R (1978) Standards for stable isotope measurements in natural compounds. Nature 271:534–536

Gonzalez Diaz E, Folguera A (2011) Análisis geomorfológico del tramo médio e inferior de La cuenca de drenaje Del rio Curri Leuvú, Neuquén. Asoc Geol Arg Rev 68:17–32

Hajdas I, Bonani G, Moreno PI, Aritzegui D (2003) Precise radiocarbon dating of late-glacial cooling in mid-latitude South America. Quat Res 59:70–78

Hogg AG, Hua Q, Blackwell PG, Niu M, Buck CE, Guilderson TP, Heaton TJ, Palmer JG, Reimer PJ, Reimer RW, Turney CSM, Zimmerman SRH (2013) SHcal13 Southern Hemisphere Calibration, 0–50,000 years cal BP. Radiocarbon 55:1889–1903

Iglesias V, Whitlock C, Markgraf V, Bianchi MM (2014) Postglacial history of the Patagonian forest/steppe ecotone (41–43S). Quat Sci Rev 94:120–135

Leger C, Tamers MA (1963) The counting of naturally occurring radiocarbon in the form of benzene in a liquid scintillation counter. Int J Appl Radiat Isot 14:65–70

Longinelli A (1984) Oxygen isotopes in mammal bone phosphate: a new tool for paleohydrological and palaeoclimatological research. Geochim Cosmochim Acta 48:385–390

Markgraf V, Whitlock C, Anderson S, Garcia A (2009) Late Quaternary vegetation and fire history in the northernmost Nothofagus forest region: MallínVaca Lauquen, Neuquen Province, Argentina. J Quat Sci 24:248–258

McCrea JM (1950) The isotopic chemistry of carbonates and a paleotemperature scale. J Chem Phys 18:849–857

Mehl AE, Zárate MA (2014) Late Glacial-Holocene climatic transition record at the Argentinian Andean piedmont between 33 and 34 ° S. Clim Past 10:863–876

Moreno PI, François JP, Villa-Martínez RP, Moy CM (2009) Millenial-scale variability in Southern Hemisphere westerly wind activity over the last 5000 years in SW Patagonia. Quat Sci Rev 28:25–38

Newnham RM, Vandergoes MJ, Sikes E, Carter L, Wilmshurst JM, Lowef DJ, McGlone MS, Sandiford A (2012) Does the bipolar seesaw extend to the terrestrial southern mid-latitudes? Quat Sci Rev 36:214–222

Panarello HO (2002) Características Isotópicas y termodinámicas de reservorio del campo geotérmico Copahue-Caviahue, provincia del Neuquén. Asoc Geol Arg Rev 57:182–194

Panarello HO, Dapeña C (2009) Large scale meteorological phenomena, ENSO and ITCZ, define the Paraná river isotope composition. J Hydrol 365:105–112

Panarello HO, Fernández J (1999) Palaeoenviromental changes in Leuto Caballo (Neuquen, Argentina) during Late Pleistocene - Holocene, Evidenced by stable isotopes on marl and Lymnaea. First results. In: Proceedings of the II South American symposium on isotope geology (IISSAGI). Argentinean Geological Service (SEGEMAR), Buenos Aires, Córdoba, Argentina, pp 418–421

Panarello HO, Sánchez EA (1985) The Kranz syndrome in the Eragrostideae (Chloridoieae, Poaceae) as indicated by carbon isotopic ratios. Bothalia 15:587–590

Panarello HO, Garcia CM, Valencio SA, Linares E (1980) Determinación de la composición isotópica del carbono en carbonatos, su utilización en Hidrogeología y Geología. Asoc Geol Arg Rev 35:460–466

Panarello HO, Sierra JL, D'Amore F, Pedro G (1992) Isotopic and geochemical study of the Domuyo Geothermal field, Neuquén, Argentina. In: proceeding of a meeting on nuclear techniques in geothermal resources investigation. San José, Costa Rica: International Atomic Energy Agency, Technical Document (TECDOC) 641: 31-56

Patané Aráoz CJP, Nami HG (2014) The First Paleoindian Fishtail Point Find in Salta Province, Northwestern Argentina. Archaeological Discovery 2:26–30

Pedro JB, van Ommen TD, Rasmussen SO, Morgan VI, Chappellaz J, Moy AD, Masson-Delmotte V, Delmotte M (2011) The last deglaciation: timing the bipolar seesaw. Clim Past 7:671-638

Rabassa J (2008) The Late Cenozoic of Patagonia and Tierra del Fuego. In: Rabassa J (ed) Developments in quaternary science, vol 11. Elsevier, Amsterdam, pp 151–204

Rabassa J, Coronato A, Martínez O (2011) Late Cenozoic glaciations in Patagonia and Tierra del Fuego: an updated review. Biol J Linn Soc 103:316–335

Renssen H, Goosse H, Fichefet T, Campin JM (2001) The 8.2 kyr BP event simulated by a global atmosphere–sea-ice–ocean model. Geophys Res Lett 28:567–570

Rozanski KP (1995) First palaeoclimatic record in arid northwest Patagonia (Neuquén, Argentina) during the Late Pleistocene and Holocene periods based on marshy shells (Lymnaea) and marl ^{18}O analyses. Final Report of coordinated research project of international atomic energy agency (CRP F34005), 54 p

Sagripanti L, Folguera A, Giménez M, Rojas Vera EA, Fabiano JJ, Molnar N, Fennell L, Ramos VA (2014) Geometry of Middle to Late Triassic extensional deformation pattern in the Cordillera del Viento (Southern Central Andes): a combined field and geophysical study. J Iber Geol 40:349–366

Sánchez N, Coutand I, Turienzo M, Araujo V, Lebinson F, Dimieri L (2014) Historia termal de la faja corrida y plegada de Chos Malal en base a nuevos datos de termocronología en trazas de fisión en apatitos. XIX Congreso Geológico Argentino. Asociación Geológica Argentina, Córdoba, pp 22–62

Shakun JD, Carlson AE (2010) A global perspective on Last Glacial Maximum to Holocene climate change. Quat Sci Rev 29:1801–1816

Sharp Z (2007) Principles of stable isotope geochemistry, 1st edn. Pearson Education Inc, New Jersey

Sugden DE, Balco G, Cowdery SG, Stone JO, Sass LC (2005) Selective glacial erosion and weathering zones in the coastal mountains of Marie Byrd Land, Antarctica. Geomorphology 67:317–334

Treese KL, Wilkinson BH (1982) Peat-marl deposition in a Holocene paludal-lacustrine basin Sucker Lake, Michigan. Sedimentology 29:375–390

Tripaldi A, Zárate MA, Brook GA, Li GQ (2011) Late Quaternary paleoenvironments and palaeoclimatic conditions in the distal Andean piedmont, southern Mendoza, Argentina. Quat Res 76:253–263

Turner JV, Fritz P, Karrow PF, Warner BG (1983) Isotopic and geochemical composition of marl lake waters and implications for radiocarbon dating of marl lake sediments. Can J Earth Sci 20:599–615

Whitlock C, Patrick J, Bartlein PJ, Markgraf V, Marlon J, Walsh M, McCoy N (2006) Postglacial vegetation, climate, and fire history along the east side of the Andes (lat. 41–42.5 S). Argentina. Quat Res 66:187–201